Multimode Polymer Chirped Fiber Bragg Grating for Shock and Detonation Velocity

YOHAN BARBARIN*, ALEXANDRE LEFRANÇOIS, VINCENT CHUZEVILLE, PASCAL HEREIL, SOFIANE ECHAOUI, LOUIS THAMIE AND JEROME LUC

CEA, DAM, GRAMAT, BP 80200, F-46500 Gramat, France
**yohan.barbarin@cea.fr*

Abstract: Shock and detonation velocities are nowadays measured continuously using long silica chirped fiber Bragg gratings (CFBG). These thin probes can be directly inserted into high-explosive samples. The use of a polymer fiber increases the sensitivity at low pressure levels when studying for instance shock-to-detonation transitions in wedge tests. 22-mm long multimode polymer CFBG have therefore been manufactured and characterized. A first detonation experiment was realized on a narrow Formex strip using such sensor. The feasibility is demonstrated and the associated uncertainties, mostly coming from the use of a multimode fiber, are discussed.

1. Introduction

Chirped fiber Bragg gratings (CFBG) are commonly used for continuous detonation wave-front position measurements in high-explosive (HE) materials recorded at high rates (>10 MHz). It was demonstrated by many groups [1-7] since almost 20 years that CFBG offer, a continuous measurement with minimal disturbance, good signal-to-noise ratio and high flexibility in the integration of the sensor. We presented many results in 2020 [8] and discussed the limitations of the silica fiber. A silica CFBG is sometimes not sensitive over its entire length especially in shock-to-detonation transitions experiments [9]. Indeed, the thin glue layer between the fiber and HE material in a narrow well attenuates the pressure level on the sensor. This affects the X-T diagram, which is the position of the wave front as a function of time. If the CFBG is not broken or at least highly compressed, the wavelength associated to the wave front position on the fiber remains in the spectrum window of the measurement. The measurement is then corrupted. From this fact, we decided to get a new fiber sensor which can be more easily broken by a shock front wave. Polymer optical fiber (POF) [10,11] with a Young's modulus of 3 GPa became an evident choice. POF had a parallel development to the silica fibers as they provide a much lower cost but it comes with higher transmission losses. POFs have thus been mostly applied for data transmission over short distances. A FBG in a POF has been already demonstrated in 1999 [12]. Few chirped FBG results were published more recently in a customized singlemode POF [13] and in a microstructured POF [14]. Since 1999, most of the efforts were as much on the development of more optimized polymer material as on applying different FBG writing technics to POF [15]. Very few companies provides commercial polymer FBG and Chirped FBG are even not available so far. Therefore, we ordered for our application customized gratings made on low-loss multimode perfluorinated CYTOP (cyclized transparent optical polymer) polymer fiber [16-17]. This first choice was driven by the low-loss properties of the fiber. The CFBG inscription is made plane-by-plane with a femtosecond laser [18]. In practice, the laser beam is swept transversely to the grating plane and across the fiber core in order to inscribe plane individually. The provider says that, compared other technics, the plane-by-plane one is more flexible. It would offer a better control of the width of the planes across the core and as well as on the depth of the grating. The fiber has a 62.5 µm core diameter with a graded index and the optical losses are in the range of 60 dB/km. For our application, only few tens of centimeters are needed so higher losses than in silica fibers can be tolerated. The

multimode (MM) behavior of the CFBG is however a new parameter for our application and this is studied in this paper. The working principle of the shock and detonation velocity measurement by CFBG is reminded and the interrogation system modified for MM fibers is presented. In section 3, an optical characterization of the Polymer Multimode CFBG (PoM-CFBG) was completed to get the parameters needed for the signal processing of the detonation veloicty. The experimentation is presented in section 4.

2. Measurement principle

The measurement principle remains the same as with a silica CFBG [8]. A CFBG is either placed along or even inside a HE material. As the detonation wave-front propagates along the HE material, the CFBG is highly shocked or even destroyed, depending on the detonation pressure. As illustrated in Fig. 1, the optical power from the source reflected back by the CFBG gradually drops from a level "1" to a level "0". The position of the detonation or shock wave-front along the fiber corresponds to a wavelength on the CFBG reflected spectrum. With the CFBG response as a function of its position, the X-T diagram (front wave position as function of time) can be calculated.

The CFBG response can be calculated from the initial reflected optical spectrum knowing the chirp rate (CR) [8]. The CR is measured with an OFDR (optical frequency-domain reflectometer) like the OBR 4600 model from Luna Technologies. It has the advantages of being non-destructive, fast, and accurate in the space domain (0.01 mm). Nevertheless, The OFDR system provides measurements as function of time, therefore the accurate fiber group index is needed to get the CR in nm/mm. The CFBG response is obtained by integrating as function of the wavelength the reflected spectrum, then the wavelength axis is linearly converted into an x-axis using the Chirp Rate value [8].

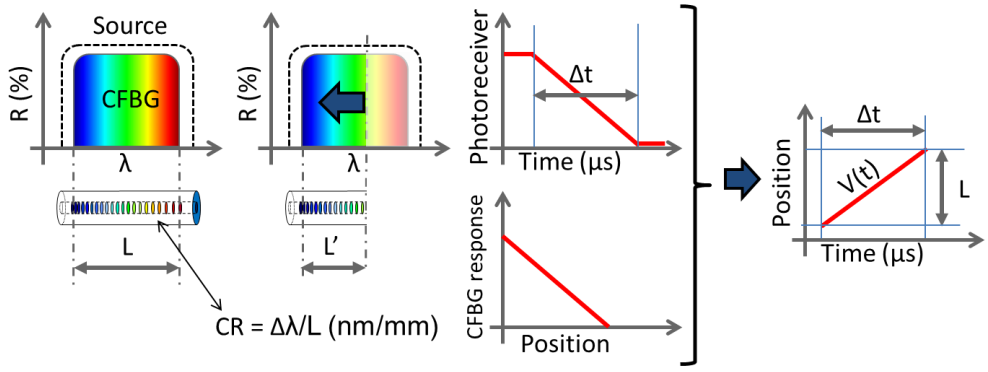

Fig. 1. Detonation velocity measurement using a chirped FBG (CFBG). In the reflected spectrum of the CFBG, a wavelength corresponds to a position along the fiber. When the fiber is shortened by the detonation, the intensity of the reflected light decreases linearly with time. This intensity corresponds to a position and then a velocity can be deduced.

The PoM-CFBG interrogator (see Fig. 2) uses a circulator with graded index 62.5-µm MM fibers and angled connectors. This fiber component is nowadays commercially available. After the single mode (SM) amplified spontaneous emission (ASE) source, all fibers are MM. The connection between the PoM-CFBG and the 20-m long MM fiber is unfortunately not angled. Indeed, angled ferrules for 500 µm bare fibers are, to our knowledge, not available. In this first experiment, the optical spectrum was measured by disconnecting the photoreceiver fiber just before the experiment. Therefore, not having a coupler between the digitizer and the optical spectrum analyzer (OSA) prevents any correction of the transmission of as function of the

wavelength for this coupler. The InGaAs wavelength response (around 1550 nm) is itself still taken into account in the signal processing [8].

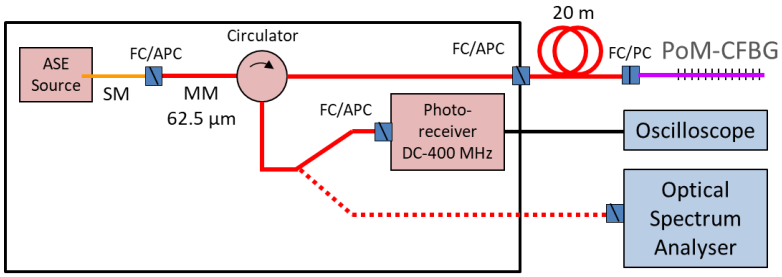

Fig. 2. Scheme of the MM interrogator of the polymer CFBG sensor. After the ASE source, all fibers are graded index silica fiber wit 62.5µm core diameter. The connection between the CFBG and the 20-m long MM fiber is not angled. The photoreceiver fiber is temporary disconnected to measure the optical spectrum.

3. Characterization of the polymer MM CFBG

The PoM-CFBGs received were very similar in terms of spectrum width on amplitude uniformity. Only the fixed optical loss at the fiber connection was varying form sample to sample. This engineering aspect can be easily improved. A PoM-CFBG was sacrificed to determine the group index of the CYTOP fiber. This fiber was mounted on a controlled translation stage and cut, step by step, to shorten it in a controlled manner. At each step, an OFDR measurement was done to measure the roundtrip time to reach the fiber extremity. As the OFDR output is SM, a passive mode convertor for MM fibers was used; it is an accessory of the OFDR system. From about hundred measurements, the CYTOP fiber group index could be calculated with low uncertainties: (1.3520 ± 0.0013) at k=2.

Next, the PoM-CFBG mounted in the following experiment was also characterized by OFDR. Again, the passive mode convertor is used. A 20-m long MM silica fiber (see Fig. 2) was necessary to reach the experiment. Fig. 3 shows the results of 10 OFDR measurements averaged. The reflectivity intensity is rather constant along the grating (blue curve) but the small spikes are deeper than with SM fibers. The chirp slope (the orange curve) is noisier than with SM silica CFBG [8]. The curve looks acceptably linear on about 80% of central part of the grating. However, the first and last 10% shows a lower slope. The noise level prevented to perform multi-sections fits with for instance three CR values depending on the position. Fits over the all range were done and the mean CR value obtained from 10 measurements is (1.029 ± 0.049) nm/mm. The uncertainties are much higher than with single mode fibers. As explained in [8], the steady-state detonation velocity uncertainties is directly linked to the CR uncertainties. The OFDR measurements provides as well the effective length (at -10 dB) of the grating: 21.8 mm. This length is significant for a laser written grating and furthermore unique in a POF. This length would perfectly cover our need for sensing the shock-to-detonation transitions in wedge tests [9]. The wedge height is indeed limited by the diameter of the gas or powder launcher used (example: 98 mm) and the 30° base angle to avoid any side release wave. For long cylinders, a length of at least 50 mm would be preferable.

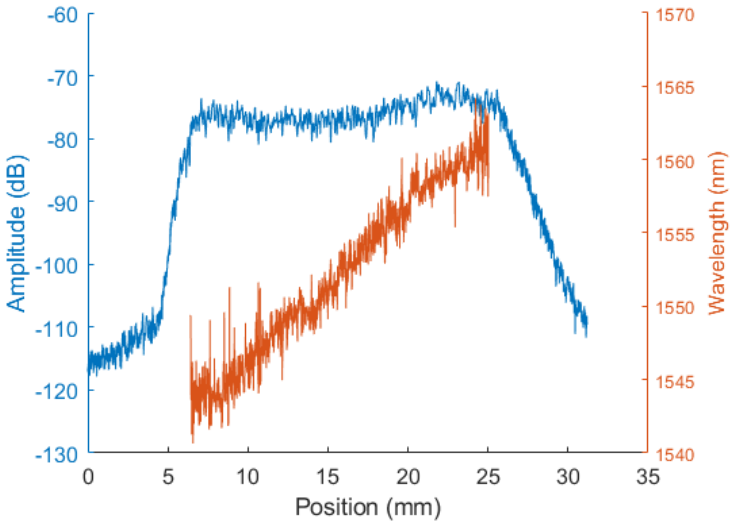

Fig. 3. Characterization of the mounted CFBG on the following experiment by OFDR. The CFBG was 20 m away and a passive mode convertor was inserted between the OFDR and the long MM fiber.

For the signal processing of the real experiment, the optical spectrum is measured to then get the CFBG response as a function of the position. It is measured using the scheme of Fig. 2, so without any mode converter. Fig. 5 shows ten optical measurements of the spectrum of the PoM-CFBG mounted on the experiment in small red dotted lines. To evaluate the variations, the blue curves show the minimums and the maximums and the black line is the mean spectrum. The variations in the spectrum are coming from the mode competition in the MM fibers. They remain even if any fiber is moving. These variations will also add uncertainties on the X-T diagram. Part of these uncertainties are hidden in the CR value measured but it can not be differentiated. In the next section, only the mean value of the spectrum will be used. The shape of the mean reflected spectrum (in a linear scale) does not have a smooth rectangular shape like in silica fiber. The spectrum shows two main regions near 1550 and 1565 nm and many spikes. As the measurement is based on the total reflectivity, the spikes are not really an issue. The shape, however, directly affects the sensor sensitivity.

The reflected spectrum is the sum of the fiber grating reflectivity and any other broadband reflections like the one at the fiber connection. The effective grating bandwidth is between 1545.1 and 1570.5 nm. In Fig. 5, it is visible with the spikes density. The grating reflected spectrum is where the spikes are clearly visible; outside, the lower intensities are as wide as the optical source. In the following section, the experimental signal on the photoreceiver will show that about 60% of the signal is coming from unwanted reflections. Therefore, the mean optical spectrum needs to be corrected to get only the PoM-CFBG reflection. This was done with Fig. 6, at the edge of the PoM-CFBG bandwidth a threshold delimits the useful signal of the grating. The dashed black curve, which delimits the estimated part coming from constant reflections, is subtracted to the mean spectrum (the red curve) to get only the optical spectrum originated in the PoM-CFBG. Without this process, the PoM-CFBG response would be wrong as well as the X-T diagram.

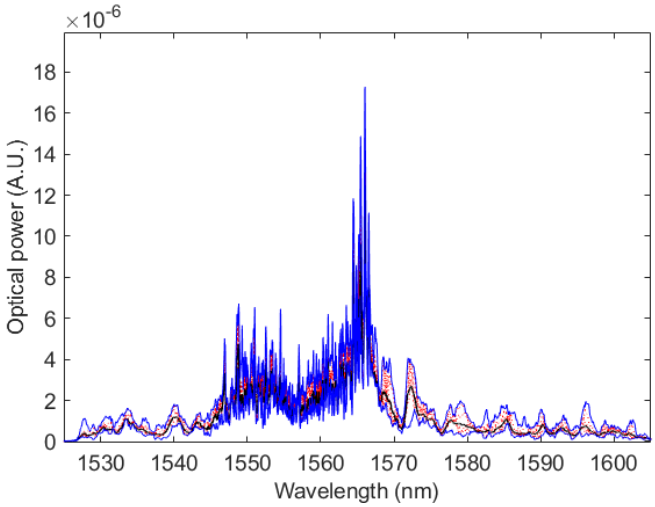

Fig. 5. Ten optical spectra in a linear scale of the PoM-CFBG mounted on the experiment (red dotted lines). The blue curves show the minima and maxima, and the black line is the mean spectrum.

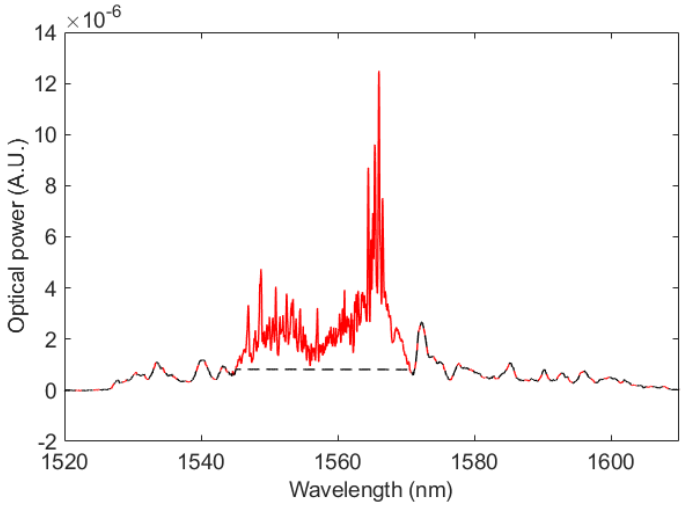

Fig. 6. Mean reflected optical spectrum (red line) and the dashed black delimits the estimated part coming from constant reflections.

4. Detonation experiment on a narrow Formex strip

In order to validate the use of a PoM-CFBG, a prototype was tested on a narrow strip of Formex explosive (89% PETN / 11% rubber binder). The strip had a smaller section than 2 x 2 mm² and the experimental setup does not allow the use of other detonation velocity sensors (pins, optical fibers…). Long silica CFBG have been previously tested, but the strip size cause important side effects and the detonation was not strong enough to always destroy the fiber and get a proper measurement. PoM-CFBG with a small diameter of 500 µm and a low young Modulus should allow a continuous measurement. The PoM-CFBG was simply glued with a thin glue layer on the surface of the Formex strip. The fiber was centered and aligned manually. For future accurate measurements, an optical control of the exact position of the fiber will be perform like we do with any sensor.

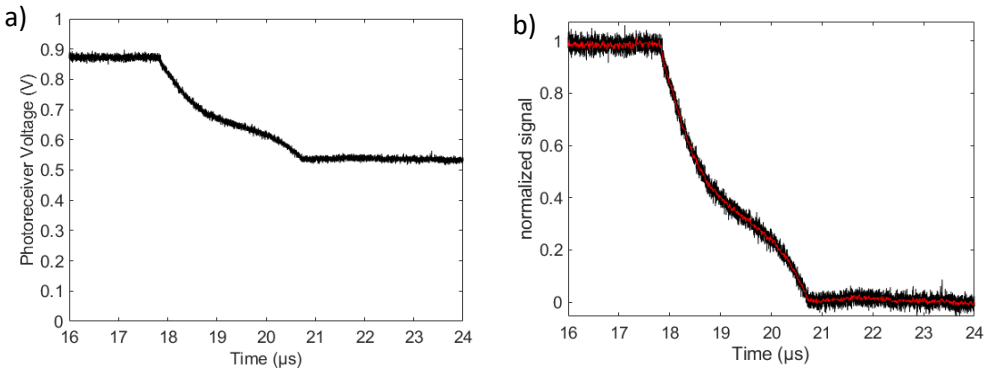

Fig. 7. a) The raw experimental signal measured at the output of the photoreceiver and b) the same signal normalized at "1" and "0" and smoothed before the signal processing.

Fig. 7. a) shows the raw experimental signal in volts of the photoreceiver. The mean amplitude between 16 and 17 µs is 87.2 mV and the mean value between 21 and 22 µs is 53.9 mV. These gives a background ratio over the total signal of 61.2%, which is very significant. This signal can easily be normalized and even smoothed (Fig. 7. b)) for the signal processing, but as mentioned in the previous section, the initial optical spectrum has to be processed to remove the background part. The processed optical spectrum was integrated as function of the wavelength and the wavelength axis converted in position using the CR values and the uncertainties. As the longer wavelengths are at the end of the fiber (see Fig. 3), these wavelengths will disappear first. Therefore, the integral calculation starts from the longer wavelengths side down to the lower wavelengths. The results are plotted in Fig. 8. Thanks to the integral step, the curve is smooth and indeed does not suffer from the spikes seen in Fig. 6. The curve is however not linear as the amplitudes in the spectrum are not constant. As mentioned previously, the sensitivity is reduced where the spectrum has lower reflectivity. The two black dashed curves show the response extrema due to the uncertainties on the measured CR value.

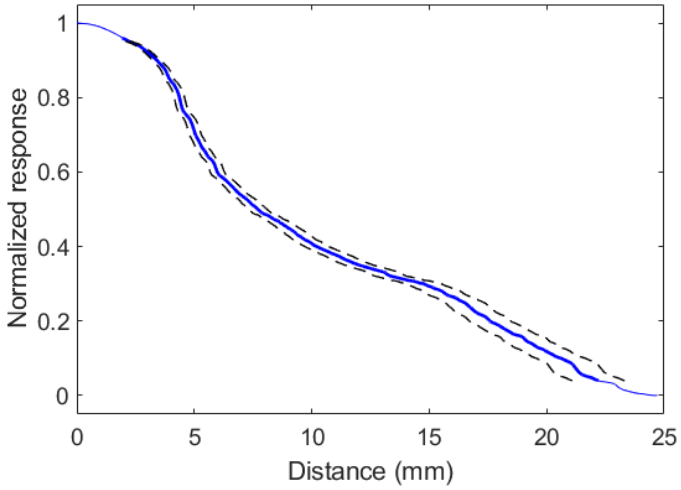

Fig. 8. PoM-CFBG response from the initial spectrum and the CR value. The two black dashed curves show the response extrema due to the uncertainties on the CR value.

The PoM-CFBG response of Fig. 8 is used to convert the normalized signal of Fig. 7.b) into position and the X-T diagram is generated. The results are plotted in blue in Fig. 9. The curve is rather linear and a fit (red curve) could be performed. The slope obtained give a steady-state detonation value of 6590 m/s. By repeating twice the calculation with the PoM-CFBG response extrema (Fig. 8), two other fits could be calculated. The slope differences provide the uncertainties on the steady-state detonation: ± 330 m/s. We would like to underline that if the signal processing is done without subtracting the constant part of the spectrum (Fig. 6), the X-T diagram obtained is not anymore close to a straight line.

The sustained detonation velocity measured by an alternative method (ultra fast video) was 6950 m/s which is within the measurement uncertainties mentioned above. It is important to notice that the video measurement is performed on a larger distance (100 mm), whereas the PoM-CFBG is more local. This 22-mm long PoM-CFBG as a sensitive shock and detonation velocity sensor has low optical losses and seems to perform correctly. The uncertainties, which are however about 5 times greater than desired, are mostly due to the multimode behavior of the PoM-CFBG and the associated fibers. It deteriorates too much the OFDR and spectral measurements to be able to get uncertainties below ± 1% (at k=2).

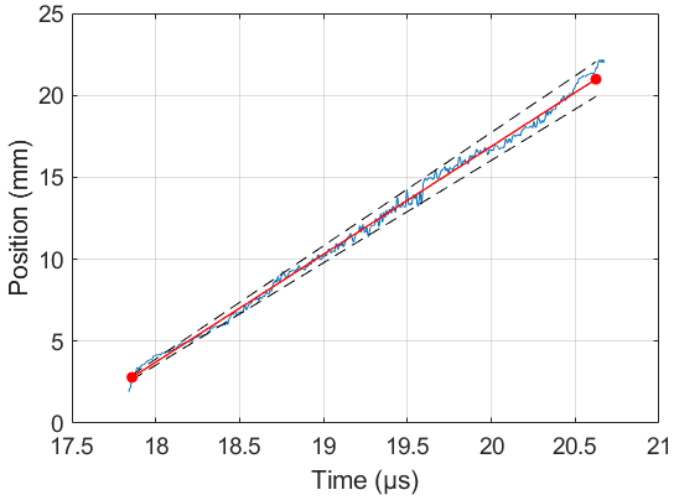

Fig. 9. X-T diagram from the PoM-CFBG measured on a Formex strip (blue curve). The red line is fitted on the data; its slopes is the steady detonation velocity. The two black dashed lines show the influence of the uncertainties of the CR value on X-T diagram.

5. Conclusion

We presented the use of a multimode polymer chirped fiber Bragg grating as a more sensitive sensor for shock and detonation velocity measurements than silica CFBG. Such sensor requires a constant chirp rate and a stable reflected optical spectrum to ensure low uncertainties in the velocity measurement. The multimode polymer chirped fiber Bragg grating made in a 62.5 µm graded index CYTOP fiber offers low optical losses, significant reflectivity and the expected mechanical behavior. The grating length (~20 mm) cover well or needs. The sample used in a detonation experiments on a narrow Formex strip suffered from high background noise but the measurement could be processed with more calculations steps. This background level could certainly be reduced by improving the connection between the silica fiber and the grating and by improving the manufacturing process. The main drawback of this polymer CFBG is the multimode fiber which creates too many instabilities and leads to higher uncertainties in the measurement. Similar polymer fibers with a 20-µm core diameter exists but they remain multimode and they are not yet directly compatible with silica fibers and components. To keep

uncertainties below ± 1% (at k=2) on a shock or detonation velocity measurement, a single-mode polymer fiber is necessary to stabilize the optical spectrum. To our knowledge, these chirped gratings have more optical losses and the linearity of the CR is difficult to guaranty.

Data availability. Data underlying the results presented in this paper are not publicly available at this time but may be obtained from the authors upon reasonable request.

Disclosures. The authors declare no conflicts of interest.

References

1. J. Benterou, C.V. Bennett, G. Cole, D.E Hare, C. May, E. Udd, S.J. Mihailov, P. Lu, "Embedded fiber optic Bragg grating (FBG) detonation velocity sensor", Proc. SPIE, 7316, 73160E, 2009.
2. E. Udd, J. Benterou, C. May, S.J. Mihailov, P. Lu, "Review of high-speed fiber optic grating sensor systems", Proc. SPIE, 7677, 76770B, 2010.
3. G. Rodriguez, R.L. Sandberg, Q. McCulloch, S.L. Jackson, S.W. Vincent, E. Udd, "Chirped fiber Bragg grating detonation velocity sensing". Rev. Sci. Instr., vol. 84, 015003, 2015.
4. S. Magne, A. Lefrançois, J. Luc, G. Laffont, P. Ferdinand, "Real-time, distributed measurement of detonation velocities inside high explosives with the help of chirped fiber Bragg gratings" Proc. SPIE 2013, 8794, 87942K.
5. Y. Barbarin, A. Lefrançois, G. Zaniolo, V. Chuzeville, L. Jacquet, S. Magne, J. Luc, A. Osmont, "Optimization of detonation velocity measurements using a Chirped Fiber Bragg Grating" Proc. SPIE, 9480, 94800S-1, 2015.
6. P. Wei, H. Lang, T. Liu, D. Xia, "Detonation velocity measurement with Chirped Fiber Bragg Grating". Sensors, 17, 2552, 2017.
7. J. Pooley, E. Price, J.W. Ferguson, M. Ibsen, "Optimized chirped fibre Bragg gratings for detonation velocity measurements" Sensors, vol. 19, 3333, 2019.
8. Y. Barbarin, A. Lefrançois, V. Chuzeville, A. Magne, L. Jacquet, T. Elia, K. Woirin, C. Collet, A. Osmont, J. Luc, "Development of a Shock and Detonation Velocity Measurement System Using Chirped Fiber Bragg Gratings", Sensors, vol. 20, 1026, 2020.
9. V. Chuzeville, G. Baudin, A. Lefrançois, M. Genetier, Y. Barbarin, L. Jacquet, J-L. Lhopitault, J. Peix, R. Boulanger, and L. Catoire, "Detonation initiation of heterogeneous meltcast high explosives" AIP Conference Proceedings 1793, 030009, 2017.
10. J. Zubia and J. Arrue, "Plastic Optical Fibers: An Introduction to their Technological Processes and Applications" Optical Fiber Technology, vol. 7, 101-140, 2001.
11. K. Peters, "Polymer optical fiber sensors - a review" Smart Mater. Struct. 20 013002, 2011.
12. G. D. Peng, Z. Xiong, P. L. Chu, "Photosensitivity and gratings in dye-doped polymer optical fibers," Opt. Fiber Technol., vol. 5, pp. 242–251, 1999.
13. C.A.F. Marques, P. Antunes, P. Mergo, D. J. Webb, P. André, "Chirped Bragg Gratings in PMMA Step-Index Polymer Optical Fiber" IEEE Photonics Technology Letters, Vol. 29, No. 6, pp. 500-503, 2017
14. R. Min, S. Korganbayev, C. Molardi, C. Broadway, X. Hu, C. Caucheteur, O. Bang, P. Antunes,D. Tosi,C. Marques, B. Ortega, "Largely tunable dispersion chirped polymer FBG" Optics Letters, Vol. 43, No. 20, pp. 5106-5109, 2018.
15. C. Broadway, R. Min, A. G. Leal-Junior, C. Marques, C. Caucheteur, "Toward Commercial Polymer Fiber Bragg Grating Sensors: Review and Applications," in Journal of Lightwave Technology, vol. 37, no. 11, pp. 2605-2615, June 1, 2019.
16. A. Theodosiou, X. Hu, C. Caucheteur, K. Kalli, "Bragg Gratings and Fabry-Perot Cavities in Low-Loss Multimode CYTOP Polymer Fiber" IEEE Photonics Technology Letters, vol. 30, No. 9, May 1, 2018.
17. A. Theodosiou, K. Kalli, "Recent trends and advances of fibre Bragg grating sensors in CYTOP polymer optical fibres" Optical Fiber Technology 54, 102079, 2020.
18. A.Theodosiou, A. Lacraz, A. Stassis, C. Koutsides, M. Komodromos, K. Kalli, "Plane-by-Plane Femtosecond Laser Inscription Method for Single-Peak Bragg Gratings in Multimode CYTOP Polymer Optical Fiber", J. Lightwave Technol. 35, 5404-5410 (2017).